Bull. Astr. Soc. India (1994) **22**, 227-245

Sizing up the universe with cosmic illusions*

S. M. Chitre
Tata Institute of Fundamental Research, Homi Bhabha Road, Bombay 400 005

Abstract. The role of gravitational lenses as valuable tools for astrophysics and cosmology is highlighted. The importance of studying gravitational lens systems for inferring the nature and distribution of gravitating matter, both luminous and dark, is examined. It is argued that cluster lenses can be profitably employed as giant cosmic telescopes to magnify remote faint objects in the Universe. It is demonstrated that with the help of observed lens system it should be feasible to attempt cosmography with a view to estimate the Hubble constant, H_0.

Key words : gravitation—cosmology

1. Introduction

The phenomenon of gravitational lensing occurs when the gravitational field of an intervening object bends the paths of light rays emitted by a remote source, in the process distorting the position, size, shape and luminosity of the background source. The basic ideas underlying gravitational deflection of light, of course, go all the way back to Newton. In recent times, the gravitational bending of starlight grazing the solar limb was measured during the total solar eclipse expedition of 1919 and its value, 1.75 arcsecond was indeed found to be twice the Newtonian value, in agreement with the prediction of general theory of relativity.

There were occasional discussions in the literature on this phenomenon by Lodge (1919), Eddington (1919) and others. Later, Einstein (1936) applied the concept of lensing of distant stars by foreground stars within the galaxy to conclude that such an event was highly improbable. It was Zwicky (1937) who discussed the phenomenon of gravitational lensing in the context of extragalactic objects; he recognized that for galaxies acting as deflectors the image-separations would be of the order of arcsecond and these should be resolvable by conventional telescopes. In the ensuing decades there was some sporadic theoretical activity due to Refsdal (1964), Liebes (1964), Barnothy (1965), Press & Gunn (1973) among others, but the real fillip to the subject of gravitational lensing was received with the discovery of the first multiply-imaged quasar system, 0957 + 561 by Walsh, Carswell & Weymann (1979). There has been considerable progress in the field, over the past dozen years, both

*Presidential address delivered at the XV meeting of the A.S.I. at Bhabha Atomic Research Centre, Bombay on March 2, 1993.

in the theoretical and observational study of gravitational lenses, and the lensed systems have come to be recognized for their diagnostic potential.

There are three broadly classified image morphologies identified so far :

(a) Multiple quasars (AGNs) : double, triple and quadruple images;

(b) Rings : extended images with ring-like morphology;

(c) Arcs : extended curved and linear features.

Table 1 summarizes some of the reasonably secure cases in each of the three classes of lens systems (cf. Blandford & Narayan 1992; Surdej and Soucail 1993).

Table 1.

Multiple quasars

Source	θ_{max} (arcsec)	Number of images	z_{source}	z_{lens}
0957 + 561	6.1	2	1.41	0.36
2016 + 112	3.8	3	3.27	1.01
1115 + 080	2.3	4	1.72	—
0142 – 100	2.2	2	2.72	0.49
0414 + 053	2 1	4	2 63	—
2237 + 031	1.8	4	1.69	0.039
1413 + 117	1.4	4	2.55	—
1422 + 231	1.3	4	3.62	—
1938 + 666	0 92	4	—	—

Radio rings

System	θ_{max} (arc sec)	z_{source}	z_{lens}
1131 + 045	2.1	—	—
1654 + 134	2.0	1.75	0.25
1549 + 304	1.7	—	0.111
1830 – 211	0.98	—	—
0218 + 357	0.30	—	—

Arcs

System	z_{source}	z_{lens}
Abell 370	0.72	0.37
Abell 963	0.77	0.21
Abell 2390	0 92	0.23
Cl 0500 – 24	0.91	0.32
Cl 1409 + 52	—	0.46
Cl 2236 – 04	1.12	0.56
Cl 2244 – 02	2.23	0 33
Abell 2163	0.73	0.20
Abell 1352	—	0.28
Cl 0302 + 17	—	0 42
Abell 1689	—	0.18
Abell 2218	—	0.17

We have to adopt certain criteria for designating a (multiply-imaged) configuration as a lensed system. For this purpose one or more of the following conditions need to be fulfilled :

(i) *Morphology* : Double, triple or quadruple images, with almost identical red-shifts, of a compact source like a distant quasar; ring-like images of an extended source such as a background galaxy

(ii) *Flux-ratios* : Nearly similar flux-ratios between images as the observing wavelength is varied

(iii) *Presence of the lense* : Detection of an intervening deflector en route to the background source

(iv) *Correlated intensity variations* : Source intensity variation reflected in various images with an appropriate time-delay

(v) *Polarization characteristic variations* : Polarization features associated with images should exhibit variations that should be correlated with an appropriate time-delay.

The foregoing criteria are, of course, intended to provide a general guide, but eventually the choice of a lens system belonging to a certain class does, however, remain somewhat subjective. There are instances of double quasars with very similar spectral characteristics which are probably not lensed objects. The double quasar 2345 + 007, with an angular separation of some 7 arcseconds, is a prototype of this class of large separation QSO pairs. In this category of QSO pairs the angular separation between quasars with nearly identical redshifts and very similar spectra, normally, exceeds 3-4 arcsec, but is smaller than, say, 10 arcsec. These pairs could either be gravitational lens systems or merely binary QSOs which happen to lie close to each other in the sky. Clearly, there is no obvious way to distinguish between gravitational lens systems and binary QSOs, except perhaps to locate a suitable intervening deflector along the sight-line and to wait, hopefully, for a time-delay between images undergoing intensity variations. It turns out that the similarity between spectral characteristics of images is not necessarily a sufficient criterion for labelling a QSO pair as a lens system.

Ever since their discovery, it has been appreciated that gravitational lenses are very valuable for studying a number of phenomena in astrophysics and cosmology. The importance of studying gravitational lens systems for inferring the nature and distribution of gravitating matter (both luminous and dark) has been widely recognized over the past decade—in fact, lensing effect is an ideal tool to search for compact as well as extended dark matter from a mass-scale of $10^6 M_\odot$ to galaxy-cluster scales. From the diverse morphologies including multiply-imaged quasars, rings and arcs that are exhibited by the observed lens systems, it should be possible to probe into structures in the Universe ranging from a scale of 10 kpc to a few tens of Mpc.

From the observed configurations, it is possible to infer the masses of lensing galaxies and galaxy-clusters. The modelling of multiple quasar systems and luminous arcs provides a handle to determine the core-radius, ellipticity and density-distribution of defective objects. The gravitational lenses such as galaxy-clusters can be profitably used as giant cosmic telescopes to provide a magnified view of the distant universe and in the process detect faint distant sources. It is feasible to attempt cosmography, specifically for estimating the Hubble constant, H_0 and the deceleration parameter, q_0, and to check the validity of standard cosmological models.

The distribution of matter in lensing objects is rarely smooth and one can hope to employ the graininess and granularity arising from individual stars (microlenses) in galactic

lenses to probe the intrinsic structure of background sources, such as angular sizes of continuum and emission line regions in quasars. Finally, the lensing can provide useful limits on the sizes of intervening Ly α clouds, reveal the presence of baryonic dark matter in the universe, detect planetary objects and black holes in the galactic and extragalactic domain and possibly even discover new exotic objects like cosmic strings. In short, gravitational lenses may give us a distorted view of the universe, but their usefulness in astronomy is beyond doubt!

2. Gravitational lens optics and mathematical formulation

The lensing phenomenon in astrophysics is a direct consequence of the gravitational bending of light. General relativity predicts that a ray of light which passes at an impact parameter, b from a point mass, M is deflected towards the body through an angle, in the weak field approximation, of magnitude

$$\theta = \frac{4GM}{c^2 b} \text{ radians.} \qquad \ldots (1)$$

The bending angle is directly proportional to the square of the characteristic radial velocity dispersion, σ and may be expressed as

$$\theta \simeq \left(\frac{4\pi\sigma^2}{c^2}\right) \simeq 1 \text{ arcsec} \left(\frac{\sigma}{250 \text{ km s}^{-1}}\right)^2. \qquad \ldots (2)$$

Originally, the emphasis in gravitational lensing theory centred around the imaging of a point source by a point mass lens. After the discovery of the gravitational lens systems, the interest shifted to multiply-imaging a point source like a quasar by an extended lens such as a galaxy or a cluster of galaxies. But there are other important scenarios, namely, the imaging of an extended source by an extended deflector en route (Saslaw, Narasimha & Chitre 1985).

The lensing geometry for a point mass source and a deflector is schematically illustrated in figure 1. Here S is the point source of radiation whose light rays are deflected by a point mass located at D and then seen by the observer at O. We project the source and image positions onto the deflector plane passing through D and which is orthogonal to the sight-line to the source. Denote the distances of the source and the image positions from D by $\vec{r}_s$ and $\vec{r}_I$, and the various distance measures as : D_s = observer-source distance, D_d = observer-deflector distance and D_{ds} = deflector-source distance. Let α be the angular displacement of the source from the deflector, D and θ_1 and θ_2 the angular displacements of the two images, I_1 and I_2 respectively from the deflector D. We shall assume throughout the concerned wavelengths to be small enough, so that the principle of geometrical optics may be adopted while describing the lensing action. Furthermore, it will be assumed that the distances involved are large compared to the impact parameter, so that for small deflections the bending angle is given by

$$\varepsilon = \frac{4GM}{c^2 |\vec{r}_I|}, \qquad \ldots (3)$$

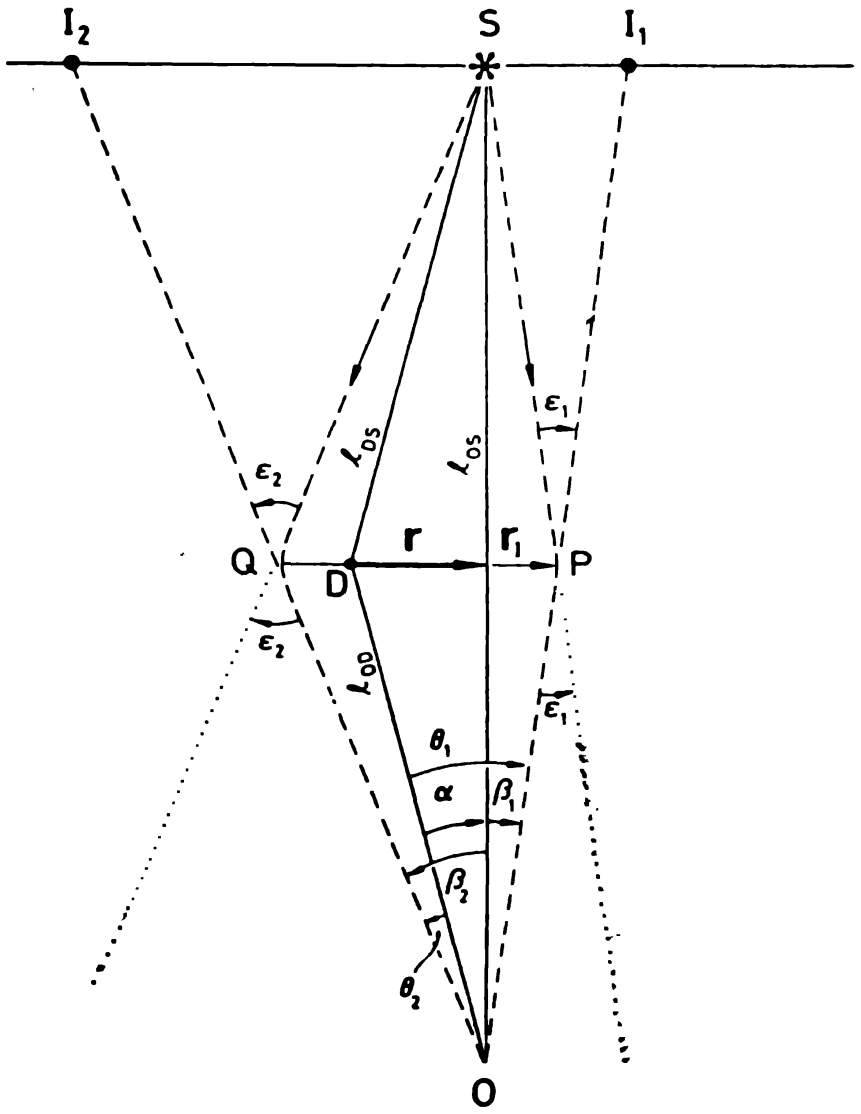

Figure 1. The schematic geometry of images of a point mass source, S and a deflector D, as seen by an observer, O.

for each ray $\vec{r}_1$ and $\vec{r}_2$. From geometrical consideration applicable to small deflections, it can be readily seen that to a very good approximation, $SI_1 \simeq \varepsilon_1 D_{ds} \simeq \beta_1 D_s$. Further noting that $\theta_1 \simeq r_1/D_d$, we can express

$$\beta_1 = \frac{\theta_0^2}{\theta_1}, \qquad \ldots (4)$$

where $\theta_0^2 = \mu/D_d^2$ and $\mu = [(4GM/c^2)\,(D_d D_{ds}/D_s)]$ is a measure of the strength of the gravitational lens of mass M. Similarly, $\beta_2 = \theta_0^2/\theta_2$ and we have the relation $\beta_2\theta_2 = \theta_0^2 = \beta_1\theta_1$. Except in the case of perfect alignment, in general $\beta_1 \neq \beta_2$ and $\theta_2 \neq \theta_1$, and we obtain $\beta_2 = \theta_1$ and $\beta_1 = \theta_2$ from the geometry and hence $\theta_1\theta_2 = \theta_0^2$.

The relation between the position of the point source, $\vec{r}_s$ and the image position, $\vec{r}_1$ is given by (cf. Saslaw, Narasimha & Chitre 1985);

$$\vec{r}_I = \vec{r}_s + \frac{\mu}{r_I^2}\vec{r}_I.$$

The scalar product with $\vec{r}_I$ gives

$$r_I^2 - r_s r_I - \mu = 0, \qquad \ldots (5)$$

which can be expressed in angular coordinates as

$$\theta^2 - \alpha\theta - \theta_0^2 = 0, \qquad \ldots (6)$$

where

$$\theta_0 = (\mu/D_d^2)^{1/2}, \quad \theta_1 - \theta_2 = \alpha.$$

The angle θ_0 denotes the angular radius of the circle of influence of the lens. It can be clearly discerned that the external image, I_1 has $\theta_1 \geq \theta_0$ and always stays outside the circle of influence, while the secondary, internal image I_2 with $\theta_2 < \theta_0$ appears within the circle. The angular radius of the circle of influence is one of the most important properties of a lens system which sets typical scale for the separation of images. In practical units, we may express the image-separation as

$$\Delta\theta \simeq 3 \text{ (marcsec) } (M/M_\odot)^{1/2} \left(\frac{(D_{ds}/kpc)}{(D_d/kpc)(D_s/kpc)}\right)^{1/2}. \qquad \ldots (7)$$

The basis of most astronomical applications of gravitational lensing is the observed angular size of these (Einstein) gravity ring-like features. Thus, in the galactic domain the gravity rings resulting from stellar mass lenses would have typical sizes of few milliarcseconds, while in the extragalactic realm, the lensing galaxies produce image-separations ~ 1 arcsec, and the galaxy-clusters yield scales ~ 1 arcmin.

The foregoing considerations are largely applicable for point source and point mass lenses. In what follows we shall analyze the lensing action in the weak field approximation for a smooth, bounded, thin transparent gravitational lens. The study of gravitational lensing of extended sources gives rise to image features that are not revealed by the lensing of a point source. In the linearized theory which is applicable to bounded sources, the bending angle for photons has a negligible component along the light path, as the distances D_s, D_d are large compared to the impact parameter. This predominantly two-component character of the bending angle enables us to adopt the complex formalism due to Bourassa and Kantowski (1975) which requires elliptical symmetry of the lens in projection. Denoting the sources position by complex number, Z_s and the image position by complex number, Z_I, the source and image positions are related by the lens equation

$$Z_s = Z_I - \frac{4GD_{eff}}{c^2} I^*(Z_I), \quad \left(D_{eff} = \frac{D_d D_{ds}}{D_s}\right). \qquad \ldots (8)$$

Here $I(Z_I)$ is the complex scattering function which incorporates the information about the lens properties like its density distribution, core radius, eccentricity etc. The object is to locate the roots of this complex equation which gives images consistent with the observed separations and intensity ratios. Clearly, for a given point in the source plane, Z_s we have corresponding points, in general more than one, in the image plane giving the locations of the images for a prescribed source position. It was demonstrated by Burke (1981) using general topological arguments that a bounded transparent gravitational lens always produces an odd number of images. Subramanian & Cowling (1986) further derived a necessary and sufficient condition for a smooth, bounded lens with elliptical symmetry to produce multiple images.

Basically there are two theoretical modelling schemes :

(i) *Direct method* : Source is represented by a minimum number of structure elements like core, knot, jet, intensity contours etc. Assuming a lens model by specifying its core radius, eccentricity, velocity dispersion etc, the ray tracing method is used to obtain the image map. The observed image-configuration is then invoked in order to refine the underlying model.

(ii) *Inverse method* : Adopting the observed image map, it is put through an assumed lens model to infer the source-structure. The intensity information of the image map is then utilized to refine the underlying model.

A successful algorithm for simulating a multiple-imaged lens system must explain the observed image-separation and intensity ratios between images, and predict the relevant time-delays. The emphasis over the past decade has been largely on the direct method to simulate the observed morphology of images (cf. Narasimha, Subramanian & Chitre 1982; Falco, Gorenstein & Shapiro 1991). Recently, there have been attempts to reconstruct the source-structure by developing inverse algorithms (Kochanek & Narayan 1992) based on the clean algorithm of radio astronomy.

A powerful theoretical formalism has been developed by Nityananda & Ostrikes (1984), Schneider (1985), Blandford & Narayan (1986), Kovner (1990) which is based on Fermat's principle, in order to study the lensing configurations. According to Fermat's principle, light rays from a source travel to the observer along a path of extremal propagation time. In the presence of an intervening deflector, the propagation time along a given light path can approximately decompose into two terms : geometrical time-delay due to the extra path-length taken by the deflected light rays and gravitational time-delay introduced by the differences in gravitational potentials along the paths. The time-delay surface may be expressed as (Cooke & Kantowski 1975)

$$\Delta t(\theta_I) = t_{geom}(\theta_I) + t_{grav}(\theta_I)$$

$$= \frac{(1+z_L)D_{eff}}{2c}(\theta_I - \theta_s)^2 - \frac{2(1+z_L)}{c^3}\int \Phi(\theta_I, z)dz, \qquad \ldots (9)$$

where Φ is the effective gravitational potential at a distance z seen by a photon passing through the position θ_I on the image plane and z_L, the lens redshift. For a given source position, θ_s, the extremal of the Fermat time-delay surface can be analyzed for obtaining the information about the image positions etc.

In the transformation from the source to the image plane (cf. equation (8)), the locus of the merging images is known as the critical curve and the corresponding locus in the source

plane is called the caustic which separates regions of different image multiplicities in the source plane. There are two generic types of caustics : folds which are lines in two-dimensional plane on which two images merge and cusps which are singular points where two folds meet. Caustics are clearly important because portions of the source that cross a caustic are highly magnified. The representative imaging of a point source and an extended source are displayed in figure 2 (cf. Narayan and Willington, 1992). In this image configuration the caustics clearly divide the source plane into 1-, 3-, 5-image regions; here the innermost caustic has four cusps joined by fold lines and a source within it is quintuply imaged. Notice the image morphology in the form of a ring or an extended arc depends on the manner in which the source is located in relation to the caustics. We shall come back to the detailed image configurations corresponding to multiple images, rings, arcs and crosses in the following section.

We have hitherto been concerned with the phenomenon of macrolensing resulting from deflectors like galaxies and clusters acting as lenses. These lenses have been assumed to have a smooth distribution of matter. In practice, however, the matter distribution has granularity in the form of individual stars and clouds. It was recognized that if an orbiting star of the deflector galaxy were to pass in front of the beam of light which has already been split by

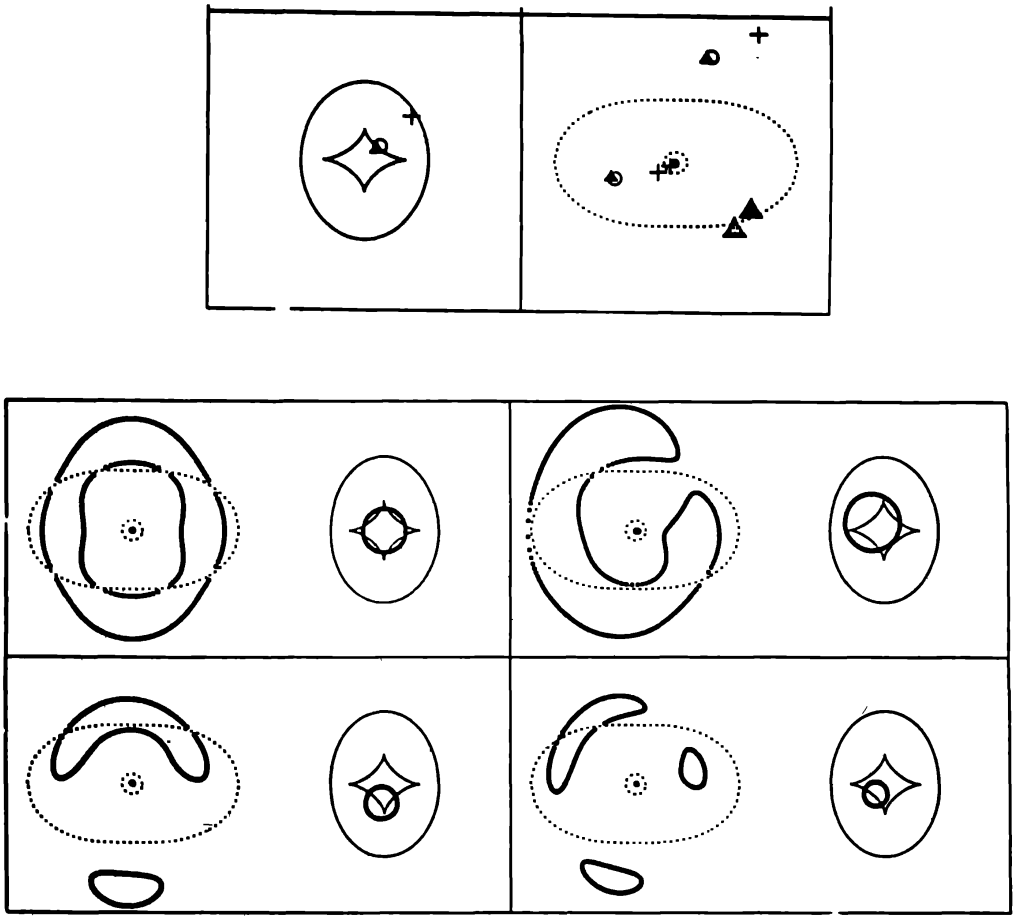

Figure 2. Typical image configuration of a point source and extended source, generated by an elliptical lens (after Narayan & Wallington 1992).

the macrolensing effect of the galaxy, the star might create additional micro-images (~ 10^{-6} arcsec separation) of a sufficiently compact source. These will be difficult to resolve, but nevertheless, they might cause a significant intensity variation (cf. Chang & Refsdal 1984; Subramanian, Chitre & Narasimha 1985; Schneider & Weiss 1987). The most dramatic effect will manifest when the source crosses a caustic resulting from the interaction of the gravitational potentials of the star and the lensing galaxy. The time scale for the observed flux variation of the image will be $t \simeq (4Gm_* D_{\rm eff})^{1/2}/v$, where v is the transverse velocity of the microlens. Thus, typically, we would expect the continuum source of a background quasar to be affected by the microlensing effect, while the larger line-emitting region will not exhibit any influence. It should not be too difficult to distinguish between changes in the image intensity induced by the intrinsic variability of the source and due to microlensing. In the former, the event is expected to be short-lived (~ weeks-months) and the light-curve will be normally peaked and there will be time-delay in the signals from various images. In the event of microlensing which should typically display a generally symmetric light curve, different images will be independently affected by microlenses.

Irwin *et al.* (1989) and Corrigan *et al.* (1991) have reported variability up to half a magnitude in the brightest image of the Huchra lens Q2237 + 031. Such a microlensing event will enable us to probe the structure of the background quasar. The contemporary ideas of the quasar-structures associate the continuum source with emission originating from a compact region of size $\simeq 10^{15}$ cm and the emission lines coming from parsec-size regions. The observations of microlensing in Q2237 + 031 are compatible with the lensing event as caused by the motion of a normal star causing the intensity variation over a period of a few months in one of the images and also leading to an upper limit of the optical continuum source. There is also a report of variability due to microlensing in 0957 + 561 (Schild & Smith 1991).

3. Cosmic mirages, arcs and rings

We shall illustrate theoretical models and simulations for some specific lens configurations.

(i) *Triple quasar PG1115 + 080*

Amongst the confirmed lens candidates the triple quasar PG1115 + 080 is an excellent, clean lens system, and we discuss here a plausible theoretical model based on the gravitational lensing of a distant quasar by an intervening galaxy. The triple quasar, discovered by Weymann *et al.* (1980) has a triangular configuration; its brightest component A has a visual magnitude of 16.2 and the other two components B and C have magnitudes 19 and 18.6 respectively. The images lie practically at the vertices of an equilateral triangle with the separations : AB = 1″.9, BC = 2″.7, CA = 2″.0. The speckle interferometric observations of the brightest component (A) have revealed that it is further resolved into two components (A_1, A_2) of comparable brightness and separated by some half an arcsecond.

This is a canonical five-image configuration of scale ~ 2″.7 produced by essentially a single-component ellipsoidal lens. The theoretical model for an assumed redshift of the lens galaxy of 0.35 is summarized in table 2 and the contours in the image plane are displayed in figure 3. The contours are depicted for a point in source plane, x = 0.10 (solid lines) and y = 0.24 (dotted lines). The intersections of these contours yield locations of the five images

Table 2. Theoretical model for the triple quasar 1115 + 080

H_0 = 50 km s^{-1} Mpc^{-1}, q_0 = 1/2

Source Position : (0″.21, 0″.08)

Lens parameters

Core-radius	:	3.25 Kpc
Velocity dispersion	:	288 km s^{-1}
Eccentricity	:	0.84
Position angle of major axis	:	90°
Cut-off radius/core-radius	:	8
Density distribution	:	$\rho \propto (r^2 + r_c^2)^{-3/2}$
Galaxy centre	:	(0, 0)
M_{nucleus}	:	$3.9 \times 10^9 M_\odot$
M_{galaxy}	:	$6.5 \times 10^{11} M_\odot$
Redshift of galaxy	:	0.35

Image properties

	Position	Amplification	Time-delay ($t - t_c$)
C	(1″.36, 0″.22)	1.97	0
B	(–0″.30, –0″.98)	–1.59	51 days
A_1	(–0″.92, 0″.58)	7.9	37 days
A_2	(–0″.58, 0″.97)	–6.0	37 days
D	(–0″.01, –0″.00)	0.002	73 days

A_1, A_2, B, C, D. Note our lens model leads to the double nature of the brightest image A, in a natural manner, with separation $\simeq$ 0″.5, between A_1 and A_2.

We notice that a substantial eccentricity in the lens galaxy is required for producing the observed five-image morphology. The predicted position of the lens galaxy turned out to be in pretty good agreement with the HST observation (cf. Crane 1992; Christian, Crabtree & Waddell 1987). Unfortunately, this system is radio quiet and hence the information on the linear magnification of its images is not forthcoming and also its optical monitoring over the past one decade has not yielded reliable time-delays. Hopefully, before long we should have a measurement of the time-delay from this system for estimating the Hubble constant to better than 20%.

(ii) *Arcs and rings*

The gravitational deflection of light rays from extended background sources reveals features that are largely absent in the image morphology resulting from the lensing action on a point-like source. The discovery of a number of luminous arcs and rings (Soucail *et al.* 1987; Lynds & Petrosian 1986; Hewitt *et al.* 1988; Rao & Subramanyam 1988; Jauncy *et al.* 1991) has further strengthened the importance of lensing of extended sources (Saslaw, Narasimha & Chitre 1985) by intervening deflectors.

The extended lens features in the form of arcs in galaxy clusters were first identified by Lynds & Petrosian (1986) and Soucail *et al.* (1987). They reported the discovery of narrow,

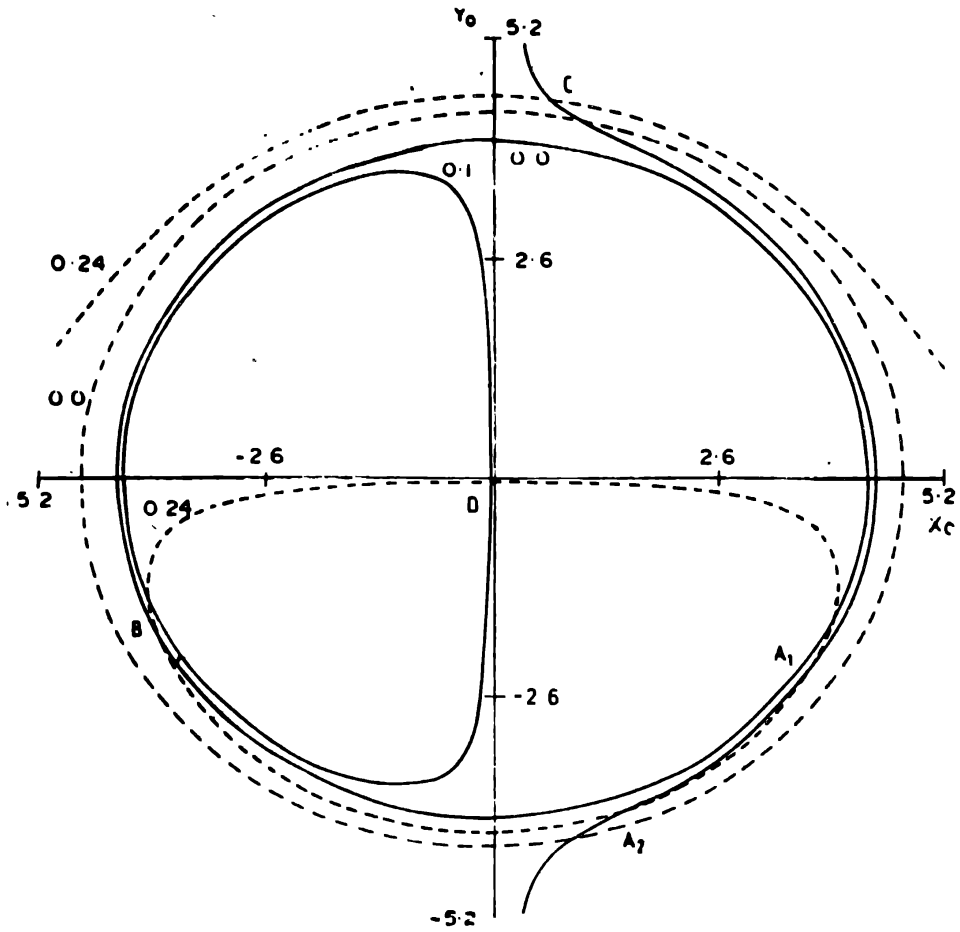

Figure 3. Image plane (x_0, y_0) showing the contours for a source position, (x, y). The five images A_1, A_2, B, C, D, are produced by the intersection of the solid contour, $x = 0.1$ with the dashed contour, $y = 0.24$.

highly elongated blue arcs extending over 20 arcsec in the cores of two rich clusters of galaxies, Abell 370 and Cl2242 – 02. Similar extended features have been reported in Abell 963 (Lavery & Henry 1988), Abell 1352, 1689, 2163 (Tyson *et al.* 1990), Abell 2390 (Pello *et al.* 1991), Cl2236 – 04 (Melnick *et al.* 1993). The redshift of the giant arc in Abell 370 was measured by Soucail *et al.* (1988) to be $z = 0.72$ and this provided a plausible explanation for the morphology of the extended arc in terms of a background galaxy being gravitationally lensed by an intervening galaxy cluster. At about this time, Fort *et al.* (1988) detected several small elongated structures in the cluster Abell 370. It is now widely believed that the arcs/arclets are manifestations of lensing phenomenon in a deep cluster potential well producing a relatively large tangential amplification in the image of an extended background galaxy (Paczynski 1987; Grossman & Narayan 1988; Narasimha & Chitre 1988). We have illustrated in figure 4 an extended arc-like morphology to simulate the giant arc in Abell 370, where a finite-sized elliptical galaxy at a redshift of $z = 0.9$ is imaged by a transparent lens in the form of a rich galaxy cluster at a redshift of $z = 0.373$. The configuration shows the large transverse magnification over a scale of 20″; the contours of the background source galaxy are indicated in figure 4 by dotted curves.

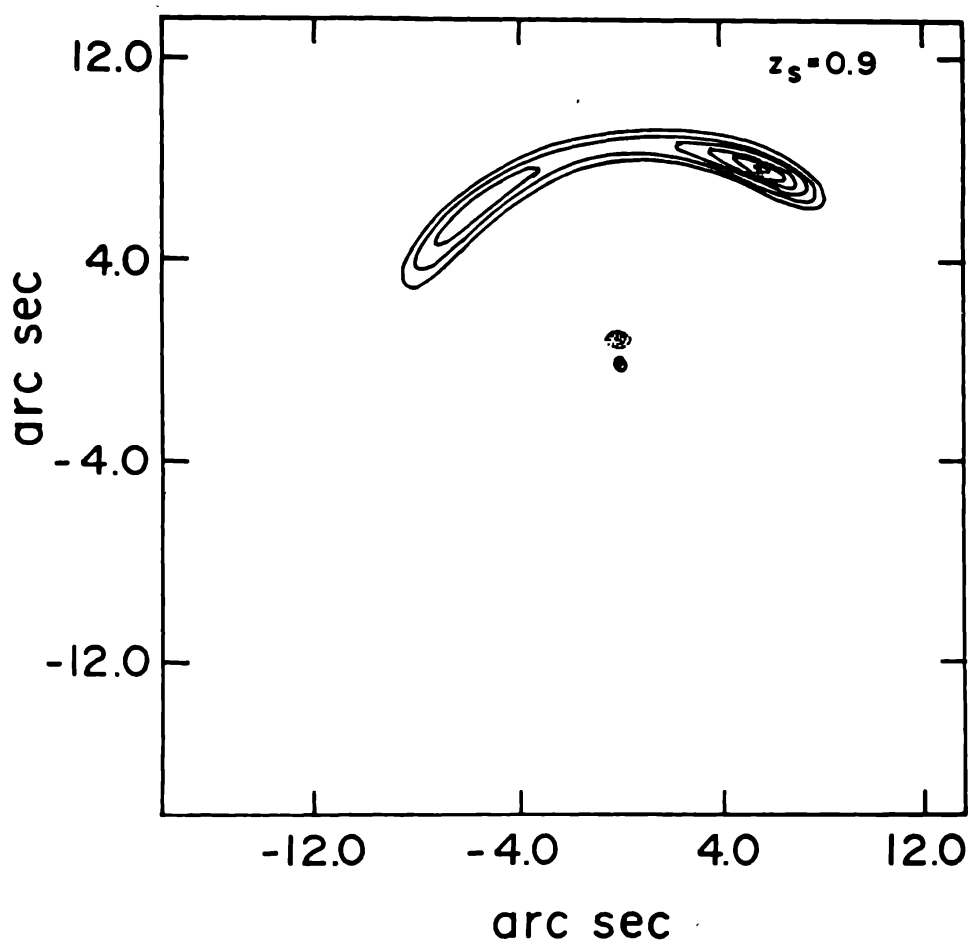

Figure 4. Tangentially amplified image of a source galaxy located at $z_s = 0.9$ by an ellipsoidal lens cluster. Dotted ellipses represent the source contours of equal intensity and the cross denotes the lens centre

Since 1986, over a dozen galaxy clusters have revealed the presence of giant arcs or arclets, and amongst these, in atleast four cases the features lying close to the cluster-centre are observed to have a linear morphology (cf. Pello *et al.* 1991; Melnick *et al.* 1993).

We note that the large tangentially amplified curved luminous arcs are produced when the background source-galaxy is located on a fold caustic. But for generating a large linear arc-like morphology we need to appeal to lip catastrophes with the extended background source-galaxy being marginally lensed by a galaxy cluster; in other words, the surface mass density Σ of the lensing cluster must be close to the critical surface density, $\Sigma_c = c^2/4\pi G D_{\rm eff}$.

We illustrate in figure 5 the source and image planes corresponding to the observed straight arc Cl2236 – 04. Here the solid curve shows the lip caustic in the source plane, while the corresponding critical curve in the image plane is indicated by the dotted ellipse. The centre of the lensing cluster at a redshift of 1.13 is marked by a cross, while one of the elliptical contours of the background source-galaxy at a redshift of 0.56 that is being marginally lensed, is exhibited intersecting the line-like lip caustic with its major axis aligned orthogonal to the caustic.

Clearly, a detailed spectroscopic study of the lensing cluster and the arcs is highly desirable. In fact, the straight arcs in Abell 2390 and Cl2236 – 04 are especially favourable

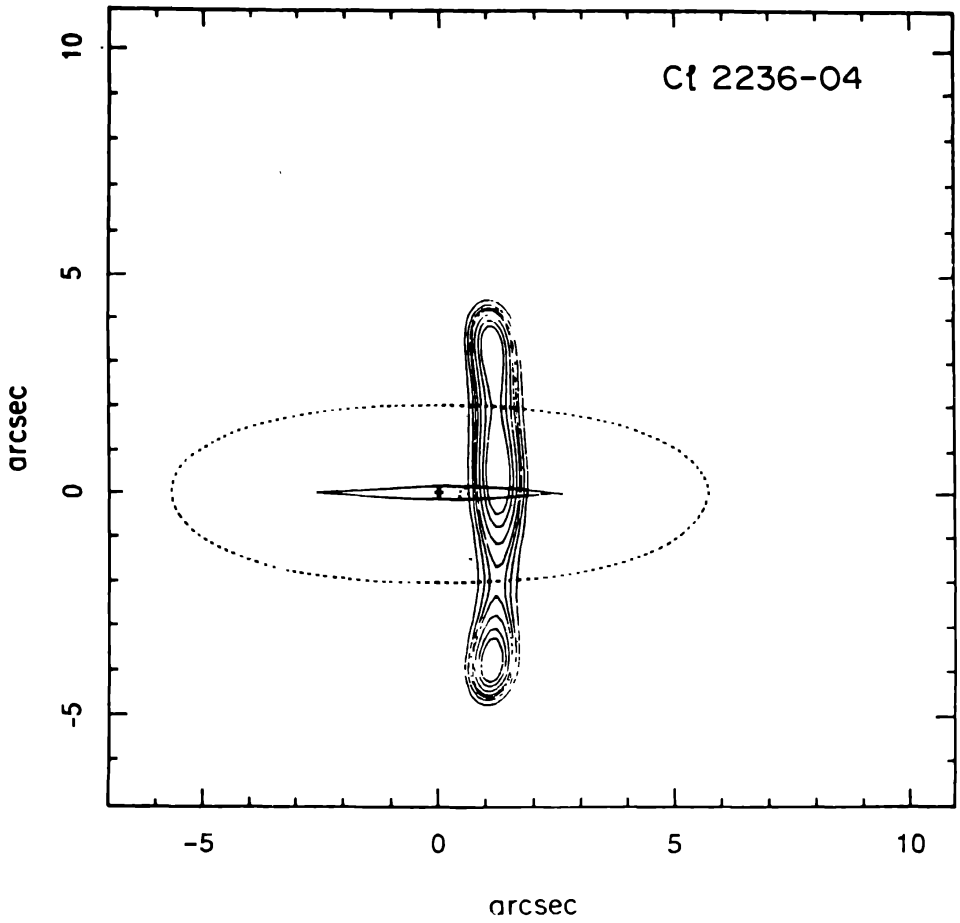

Figure 5. Morphology of the straight arc Cl2236-04, where the solid curve shows the lip caustic in the source plane, while the corresponding critical curve in the image plane is indicated by the larger dotted ellipse The cross represents the lens centre and the background source is shown by a broken ellipse lying practically inside the lip caustic.

for mapping the velocity field and brightness distribution associated with the background source-galaxy. Equally, the morphology of these extraordinary linear structures should enable us to constrain the surface mass distribution and gravitational potential of the lensing cluster.

A similar image configuration of partial or near complete ring-like images with angular extent of arcseconds results when background radio sources are lensed by a radio-quiet, intervening deflector in the form of a galaxy. A typical ring-like morphology is illustrated in figure 6 which shows schematically how a background source consisting of a bright nucleus and surrounding fuzz are imaged by an intervening galaxy lens to produce an almost complete ring configuration with multiple bright regions. Here the source is indicated by circular contours of varying intensity and the cross denotes the centre of the lens galaxy. A similar scenario is sufficient to account for the qualitative understanding of the two radio rings MG1131 + 0456 and MG 1634 + 1346 (Hewitt *et al.* 1988; Langston *et al.* 1989). Thus, the intrinsic source-structure of MG1131 + 0456 may be a compact core accompanied by two radio lobes, one of which could fall directly behind the lens galaxy to get imaged into a radio ring. The compact core could be situated near enough to the lens to be imaged into $A_1 - A_2$ and B, and the second lobe would be too far to be affected significantly by the lens.

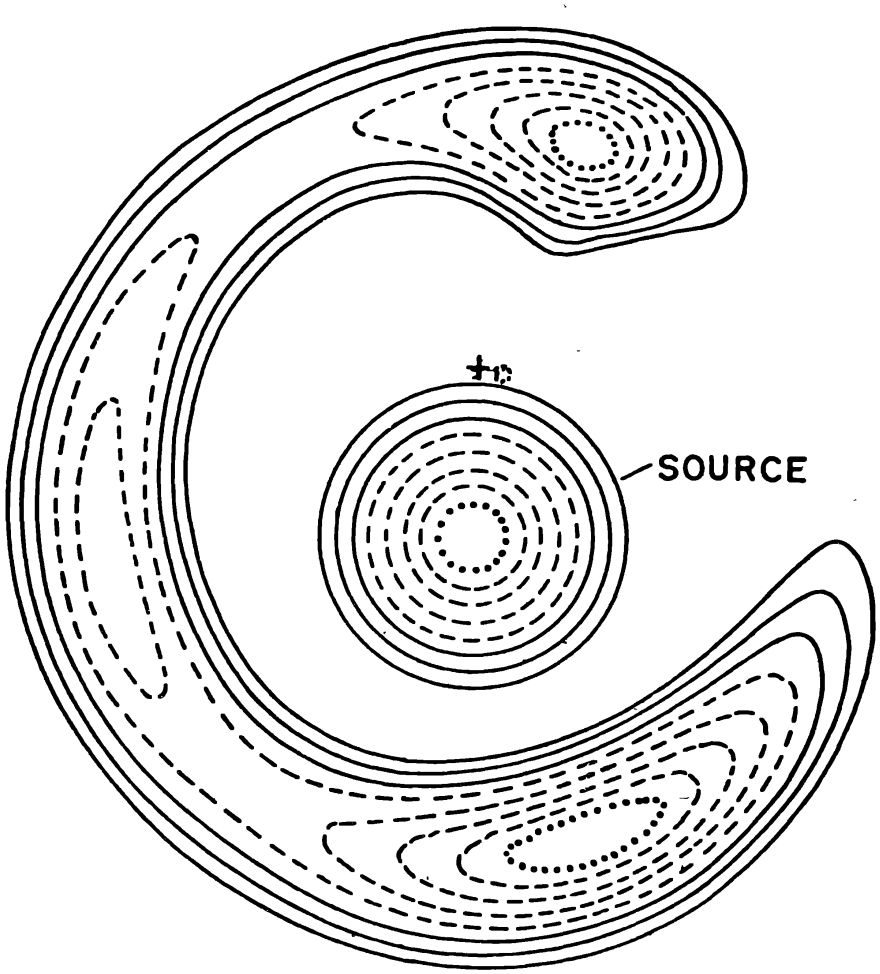

Figure 6. Schematic image morphology resulting from a background source made up of a bright nucleus with a surrounding fuzz, lensed by an intervening object to produce an almost complete ring The circular contours indicate the source of varying intensity and the cross denotes the centre of the deflector.

Even though this ring contains a doubly-imaged compact radio core which will, hopefully, turn out to be variable and in the process furnish us with a time-delay measurement, there is no knowledge of the redshift of either the source or the lens. On the other hand, for the radio ring MG1634 + 1346, both the redshifts of the source and the lens are known, one of the radio lobes of the high redshift (z = 1.74) quasar is imaged into a ring-like morphology while the central component is only singly imaged by a low redshift (z = 0.254) galaxy en route.

The Ooty object, 1830-211 is an unusually strong (~ 10 Jy) flat-spectrum double radio source with ~ 1 arcsecond separation having a ring-like morphology. It can be modelled assuming a source, lying for most part in a three-image region bounded by radial caustic, made up of dominant core and a knot with a highly bent jet on a scale of fraction of an arcsecond. The schematic model of Nair, Narasimha & Rao (1993) is displayed in figure 7. Nair (1993) has pointed out that since almost all compact flat-spectrum radio sources show variability in the linearly polarized flux as well as in the orientation of the polarization vector, it might be possible to use the polarization variability between images of 1830-211 for time-delay measurements.

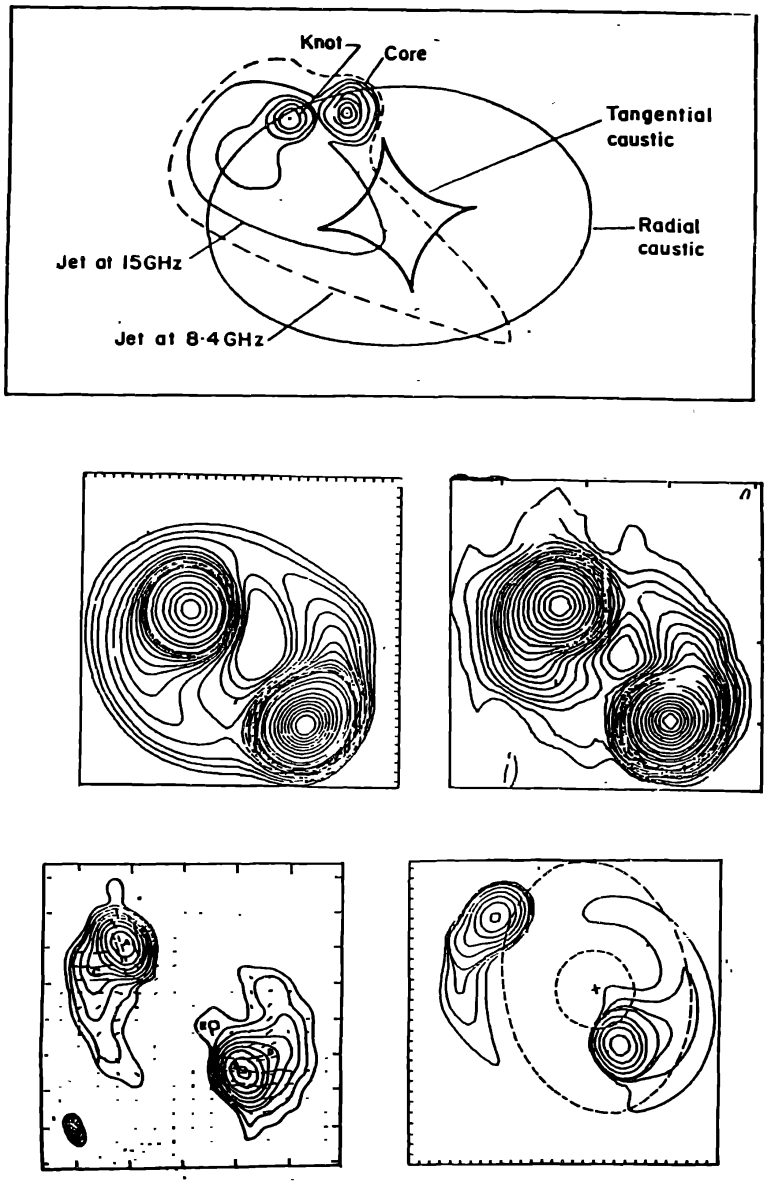

Figure 7. Ring-like configuration for the Ooty object 1830-211 can be reproduced by assuming a source made up of a dominant core, a knot and a highly bent jet, lying mainly in a 3-image region bounded by a radial caustic generated by the lens galaxy

4. Sizing up the universe

4.1. *Gravitational lensing and dark matter*

Gravitational lenses have long held the promise of locating dark matter in the universe, and finding out how it is distributed in the potential wells of galaxies and rich galaxy clusters. Since lenses are particularly sensitive to the total mass distribution, they are useful in mapping both the luminous and dark matter present in deflectors. There are also a number of relatively large separation, possible double-imaged quasars like 2345 + 007 and 1635 + 267, which have remarkably similar spectral properties (cf. Weedman *et al.* 1982; Djorgovski

& Spinrad 1984). It is, of course, not unlikely that these two systems may conceivably be quasar pairs that happen to be spatially correlated (Blandford & Kochanek 1987). Recent observations, however, appear to strengthen the proposal that these two systems are examples of the phenomenon of dark matter gravitational lensing. (Turner *et al.* 1988; Tyson *et al.* 1986; Weir & Djorgovski 1991; Steidel & Sargent 1991). It also appears from theoretical considerations (Narasimha & Chitre 1989) that there is a compelling need to invoke the assistance of an additional mass component around the lens galaxy either in the form of a dark halo or as yet undetected compact core of a galaxy cluster in order to reproduce the observed image configurations of these tentative lens systems : 2345 + 007 and 1635 + 267. But for such an explanation to become more tenable, we have to look for some incontrovertible evidence for multiple imaging like time-delay or the presence of lensing agents.

Narasimha & Chitre (1989) have proposed that massive underluminous galaxies with dark halos may be responsible for lensing action in some of the systems where the deflecting agents are being elusive. It was speculated that there might be present in the universe large-size, high mass ($\geq 10^{13}\, M_{\odot}$) low surface brightness (LSB) galaxies at low to moderate redshifts which could serve as dark lenses—these objects could only be detected by their gravitational influence on distant background sources. The extended images of a high redshift galaxy are liable to be overwhelmed by the light of the foreground lens galaxy. A 'dark' LSB galaxy, on the other hand, is unlikely to mask the arc-like or ring-like image morphology and it is tempting to speculate that perhaps highly underluminous galaxies in which there has been insufficient star formation and which contain large amounts of neutral hydrogen gas may be the dark lensing agents for some of the candidate gravitational lens systems. The presence of large quantities of neutral hydrogen gas is certain to give rise to radio emission at 21 cm with an expected radio output of $\sim 6 \times 10^{35}$ erg s^{-1}, implying the radio flux ~ 16 mJy for an assumed redshift of the lens galaxy $z = 0.7$ (cf. Narasimha & Chitre 1989). A definitive test for such a dark matter lens would be a copious amount of 21 cm emission in the frequency band 500 to 1400 MHz (for the range of redshifts $z = 0.5$-1.5) and Ly α absorption at the same redshift.

The study of giant luminous arcs in rich galaxy clusters (e.g. Abell 370) and the presence of several faint arclets elongated tangentially in relation to the cluster-centre, reinforce the idea that perhaps dark matter is not necessarily clustered around galaxies, but rather it is distributed smoothly throughout the cluster and is perhaps centred around the luminous matter distribution. Tyson *et al.* (1990) have detected several arclets in the cluster Abell 1689, from which they attempted to infer a map of the dark matter present in the clusters. Thus, the detection of several tens of arclets in rich clusters will doubtless provide us a valuable diagnostic not only of the distribution of gravitating mass (luminous + dark) in clusters, but also the redshift distribution of background galaxies that are being lensed.

From the observed gravitational lens systems it is reasonable to draw the following conclusions about the distribution of matter :

(i) The distribution of gravitating matter in the Universe does not necessarily follow the distribution of light; in some of the galaxy clusters, the centre of dark mass is not even coincident with the centre of visible matter.

(ii) There is a compelling reason to believe that some of the lensing objects are probably made of dark matter.

(iii) The lensing objects have very compact, or even singular cores.

4.2. *Time delay measurement*

The transit time of photons from a distant source to the observer depends on the path taken by the light rays. An important consequence of the gravitational lensing action due to intervening deflector en route is that if the intensity of the unlensed background source varies with time, these variations will not be reflected in all the images simultaneously, but rather with a relative time delay between different images. This can be expressed as a combination of a delay caused by the difference in geometrical path lengths of the light rays and a delay resulting from the different gravitational potential wells which the photons sample. The effective time-delay, expressed by equation (9), is inversely proportional to the Hubble constant, H_0, for a specified value of the deceleration parameter (cf. Refsdal 1964; Cooke & Kantowski 1975; Schneider 1985).

The very first gravitational lens system detected, 0957 + 561 is luckily a variable source, both in the optical and radio bands. The system has been monitored for over a decade for measuring the fluxes from components *A*, *B*. The light curves have been correlated by a number of investigators (Schild 1990; Press *et al.* 1992) to give a time-delay of order 540 ± 12 days. However, the time-delay estimates are rendered uncertain because of the complications arising from the variability contributed by possible microlensing effects.

We can determine the Hubble constant, H_0 from the time-delay measurements provided, of course, we have a good knowledge of the redshifts of the source and the lens, and the mass distribution, the ellipticity, linear scale and orientation of the lens. Unfortunately, the system 0957 + 561 is somewhat complicated because of the presence of two lensing agents—giant elliptical galaxy and the cluster. Falco, Gorenstein & Shapiro (1991) assume the velocity dispersion for the lens galaxy of ~ 390 km s^{-1} in their theoretical model to give a Hubble constant of 55 km s^{-1} Mpc^{-1} (for $q_0 = 1/2$) although there are considerable uncertainties in this estimate of H_0. We have to await the time-delay measurement from a 'clean' lens system like the triple quasar 1115 + 080 to yield a more reliable and accurate value of the cosmological parameters.

The radio rings (e.g. MG1131 + 0456, MG1654 + 1346) offer another possibility of deducing a time-delay if the doubly imaged compact core turns out to be variable. Unfortunately, it has not been possible to measure the redshifts of the source and the lens for the radio ring MG1131 + 0456, while the central component of the source MG1634+1346 is only singly imaged (Blandford 1990).

An exciting possibility is to look for a transient source (e.g. a supernova) in the background source galaxy. Suppose a supernova goes off in the distant galaxy which is being lensed by a foreground rich cluster. The supernova event will appear in the distant multiply imaged regions of the arc-like image morphology of the lensed galaxy, but with a time-delay of order 3-8 months, depending on the location of the images. With a reasonable idea about the cluster mass distribution, we may be able to estimate the value of H_0.

It is also tempting to speculate that straight arc morphologies observed in the cores of rich clusters (e.g. Abell 2390, Cl 2236-04) could serve as valuable distance indicators, provided, of course, we have a measurement of their velocity dispersion (or, the mass) and the core-radius to better than 10%. Since the production of a linear feature necessarily involves the phenomenon of marginal lensing, with the surface mass density, Σ, of the lensing cluster close to, but just above the critical density, $\Sigma_c = c^2/4\pi G D_{eff}$, we can reasonably adopt the equation, $\Sigma = \Sigma_c$ to solve for D_{eff} and hence infer H_0 for a specified value of q_0.

5. Conclusions

It is clear that gravitational lenses have a considerable impact on a variety of astrophysical phenomena. Gravitational lensing is evidently capable of probing the distribution of all gravitating matter—luminous and dark—that is present in galaxies and clusters. The lensing phenomenon can help us to infer the mass distribution in lensing galaxies and clusters and also to deduce other parameters like their core-radius and eccentricity. The lensing also enables us to probe the structure of remote quasars, particularly, the continuum and emission line regions. The cluster lenses can serve as natural telescopes and act as magnifiers for faint distant galaxies lying behind the lensing clusters. The lensing action offers us a valuable diagnostic to surmise the nature of dark matter, particularly, whether it consists of discrete compact objects (e.g. brown dwarfs, black holes) or is made up of a sea of weakly interacting massive particles. We can attempt to undertake cosmography with the help of gravitational lensing and hope to determine the cosmological parameters like the Hubble constant, and also check the validity and internal consistency of cosmological models. Finally, lensing might even reveal new exotic objects such as cosmic strings. In short, we have now an astronomical tool which has immense potentialities to enlarge our horizons in astrophysics and cosmology.

Acknowledgement

It is a pleasure to express my grateful thanks to my colleague, Dr Narasimha, for innumerable discussions and enlightening comments.

References

Barnothy J., 1965, AJ, 70, 666

Blandford R D , 1990, Q J R. astro. Soc., 31, 305

Blandford R D , Narayan R., 1986, ApJ, 310, 568.

Blandford R. D., Narayan R., 1992, Ann. Rev. Astr. Ap , 30, 311.

Blandford R. D., Kochanek C. S., 1987, ApJ, 321, 658.

Bourassa R R., Kantowski R., 1975, ApJ, 195, 13

Burke W. L., 1981, ApJ, 244, L1

Chang K., Refsdal S , 1985, A&A, 132, 168.

Christian C. A., Crabtree D., Waddell P., 1987, ApJ, 312, 45.

Cooke J. H., Kantowski R , 1975, ApJ, 195, L11

Corrigan R T , Irwin M. J., Arnaud J , Fahlmar G. G., Fletcher J. M., 1991, AJ, 102, 34.

Crane P., 1992, in · Gravitational Lenses (Proc. Hemburg Conference), 112

Djorgovski S, Spinrad H., 1984, ApJ, 282, L1

Eddington A. S., 1919, Observatory, 42, 119.

Einstein A., 1936, Science, 84, 506.

Falco E. E , Gorenstein M. V., Shapiro I. I., 1991, ApJ, 372, 364.

Fort B , Prieur J. L , Mathez G., Mellier Y , Soucail G., 1988, A&A, 200, L17.

Hewitt J. N., Turner E. L , Schneider D. P., Burke B. F., Langston G I , Lawarence C. R., 1988, Nature, 333, 537

Hewitt J. N., Turner E L., Schneider D. P., Burke B. F , Langston G. I , Irwin M. J., Webster R. L., Hewett P C., Corrigan R. T., Jedrzejewski R L., 1989, AJ, 98, 1989.

Jauncey D L. *et al* , 1991, Nature, 352, 132

Kochanek C. S , Narayan R , 1992, ApJ, 401, 461.
Kovner I., 1990, ApJ, 351, 114
Lavery R J., Henry J. P., 1988, ApJ, 329, L21
Liebes S. 1964, Phys Rev., 133, B835
Langston G I , Schneider D. P., Conner S., Carilli C. L., Lehar J., 1989, AJ, 97, 1283.
Lodge O., 1919, Observatory, 42, 365.
Lynds R., Petrosian V , 1986, BAAS, 18, 1014.
Melnick J , Altier B , Gopal Krishna, Giraud E , 1993, A&A, 271, L5.
Nair S., 1993, Ph.D. Thesis, Bombay Univ.
Nair S.., Narasimha D , Rao A P , 1993, ApJ 407, 46
Narasimha D., Subramanian K , Chitre S M , 1982, MNRAS, 200, 941
Narasimha D , Chitre S. M., 1988, ApJ, 332, 75.
Narasimha D., Chitre S. M , 1989, AJ, 97, 327.
Narayan R , Willington S., 1992, ApJ, 399, 368.
Nityananda R., Ostriker J. P , 1984, JApA, 5, 235.
Paczynski B , 1987, Nature, 325, 572.
Pello R , Le Borgne J F , Soucail G., Mellier Y., Sanahuja B , 1991, ApJ, 366, 405.
Press W. H., Gunn J E., 1973, ApJ, 185, 397.
Rao A. P., Subramanyan R., 1988, MNRAS, 231, 229.
Refsdal S , 1964, MNRAS, 128, 295.
Saslaw W. C., Narasimha D., Chitre S. M., 1985, ApJ, 292, 348.
Schild R. E., 1990, AJ, 100, 1771.
Schild R E , Smith R. C., 1991, AJ, 101, 813.
Schneider P., Weiss A , 1987, A&A, 171, 49
Schneider P., 1985, A&A, 143, 413.
Soucail G , Fort B., Mellier Y., Picat J.-P., 1987, A&A, 172, L14.
Soucail G., Mellier Y , Fort B , Mathez G , Cailloux, M , 1988, A&A, 191, L19
Steidel C. C , Sargent W. L. W., 1991, AJ, 102, 1610.
Subramanian K , Chitre S. M., Narasimha D., 1985, ApJ, 289, 37
Subramanian K., Cowling S. A , 1986, MNRAS, 219, 333.
Surdej J., Soucail G., 1983, in : Gravitational Lenses in the Universe (Proc 31st Liege Colloquium)
Tyson J. A., Valdes F., Wenk R. A , 1990, ApJ, 349, L1
Tyson J. A., Seitzer P., Weymann R J., Foltz C., 1986, AJ, 91, 1274
Turner E L., Hillenbrand L. A., Schneider D. P., Hewitt J N., Burke B F., 1988, AJ, 96, 1682.
Weir N., Djorgovski S., 1991, AJ, 101, 66
Walsh D., Carswell R F., Weymann R. J., 1979, Nature, 279, 381.
Weedmann D. W., Weymann R. J., Green R. F , Heckman T. M., 1982, ApJ, 255, L5.
Weyman R. J., Latham D., Angel J. R P., Green R. F., Liebert J. W , 1980, Nature, 285, 641
Zwicky F., 1937, Phys. Rev. Lett., 51, 290